Geomagnetic field morphologies from a kinematic dynamo model

David Gubbins & Graeme Sarson

Department of Earth Sciences, Leeds University, Leeds LS2 9JT, UK

THE Earth's magnetic field is generated by flow of liquid iron in the outer core, acting as a dynamo. In the simple kinematic theory a fluid flow is prescribed and tested for its ability to generate magnetic field, no account being taken of the forces required to drive the flow. Although incomplete, kinematic theory gives valuable insight into the more difficult dynamical problem and produces field morphologies which can be compared with observations. We are attempting a comprehensive study of three-dimensional kinematic dynamo action for a class of fluid flow typical of that driven by convection (G.S. and D.G., manuscript in preparation), and

have already found similarities between steady dipole solutions and the geomagnetic field[1]. Here we examine the effect of meridian circulation in determining the stability of steady and oscillatory solutions. The magnetic field morphology on both sides of the stability boundary is determined by magnetic flux concentration by downwelling fluid[2]. The oscillatory dipole reverses polarity through the appearance and poleward migration of patches of reversed flux, similar to those seen in today's geomagnetic field[3]. Virtual geomagnetic poles computed from the reversing field follow paths that are concentrated along the longitudes of maximum flux, suggesting a link with recent palaeomagnetic results[4–7].

The magnetic field **B** obeys the induction equation

$$\frac{\partial \mathbf{B}}{\partial t} = R_m \nabla \times (\mathbf{v} \times \mathbf{B}) + \nabla^2 \mathbf{B} \qquad (1)$$

where **v** is the fluid velocity, $R_m = \mathscr{U} c \mu_0 \sigma$ the magnetic Reynolds number, $\mathscr{U}$ the velocity scale, c the linear dimension (core radius for the Earth), σ the electrical conductivity and μ_0 the magnetic permeability of free space. **v** is prescribed, so that equation (1) is linear in **B** and has solutions that vary in time, t, as $\exp(p + i2\pi f)t$. Dynamo action occurs if we can find a critical value of R_m, R_m^c, such that the growth rate $p \geq 0$ (**B** does not decay with time). At marginal stability $p = 0$ and if $f = 0$ the solution is steady, otherwise it is oscillatory with frequency f.

Although this kinematic approach cannot reproduce complicated time variations such as irregular polarity reversals, it can increase our understanding of the physical processes occurring in dynamo action at a time when full simulations of the dynamical behaviour of a model of the Earth's core are not feasible. For example, the Parker–Levy[8–10] reversal mechanism is based implicitly on kinematic results.

Despite its mathematical simplicity, the kinematic dynamo problem poses severe numerical difficulties: apparent "solutions"[11,12] have subsequently been shown[13–15] to be numerical artefacts. Somewhat greater success was achieved with α-effect dynamos, which in the geophysically relevant Braginsky[16] formulation involves averaging in longitude and taking the limit $R_m \gg 1$ to yield equations for the axisymmetric field $\bar{\mathbf{B}}$:

$$\frac{\partial \bar{\mathbf{B}}}{\partial t} = R_m \{\nabla \times (\omega \hat{\boldsymbol{\phi}} \times \bar{\mathbf{B}}_p) + \nabla \times [(\bar{\mathbf{v}} + \bar{\mathbf{v}}_{ep}) \times \bar{\mathbf{B}}] + \nabla \times (\alpha \bar{B}_\phi \hat{\boldsymbol{\phi}})\} + \nabla^2 \bar{\mathbf{B}} \qquad (2)$$

where subscript p denotes the meridian component, $\hat{\boldsymbol{\phi}}$ is a unit azimuthal vector, ω is the differential rotation, overbars denote axisymmetric quantities, α is related to the helicity $\mathbf{v} \cdot \nabla \times \mathbf{v}$, and $\bar{\mathbf{v}}_{ep}$ is an 'effective meridian circulation' which, like α, is derived from products of components of the original flow. Successful numerical solutions to the simpler $\alpha\omega$ equation (2) have been extensively documented[17,18], including some dynamical studies[19–22], but they cannot produce non-axisymmetric morphology for comparison with the geomagnetic field.

We have therefore conducted a series of calculations on three-dimensional (3D) kinematic dynamos using the numerical method of Bullard and Gellman[11] as implemented by Gubbins[14], but carried to higher numerical accuracy than previously. Three-dimensional calculations and Braginsky limit calculations have been carried out in parallel; correspondence between the two systems allows us to have confidence in the accuracy of our solutions.

Our basic fluid flow is that chosen by Kumar and Roberts[23], with the general form:

$$\mathbf{v} = \mathbf{t}_1^0 + \varepsilon_1 \mathbf{s}_2^0 + \varepsilon_2 \mathbf{s}_2^{2s} + \varepsilon_3 \mathbf{s}_2^{2c}$$

where

$$\mathbf{t}_l^{mc} = \nabla \times [t_l^{mc}(r)\, P_l^m(\cos\theta) \cos m\phi \hat{\mathbf{r}}]$$

$$\mathbf{s}_l^{mc} = \nabla \times \nabla \times [s_l^{mc}(r)\, P_l^m(\cos\theta) \cos m\phi \hat{\mathbf{r}}]$$

Here $P_l^m(\cos\theta)$ is an associated Legendre function, $\hat{\mathbf{r}}$ a unit radial vector, and the second superscript denotes cos or sin dependence on ϕ. The $\mathbf{t}_1^0$ harmonic provides differential rotation (the ω-effect), the s_2^0 meridian circulation, and the s_2^2 harmonics overturning. R_m is scaled with the differential rotation; the parameters ε_i give the relative importance of other harmonics. The case $\varepsilon_1 = 0$ corresponds to Lilley's[12] dynamo with a different radial dependence prescribed. The radial dependence used here is: $t_1^0(r) = r^2(1-r^2)$, $s_2^0(r) = r^6(1-r^2)^3$, $s_2^{2s}(r) = r^4(1-r^2)^2 \cos(nr)$, $s_2^{2c}(r) = r^4(1-r^2)^2 \sin(nr)$; we illustrate our results with $n = 3\pi$, corresponding to convection with three cells in radius. Comparable results to those presented here have been obtained for different values on n (G.S. and D.G. manuscript in preparation).

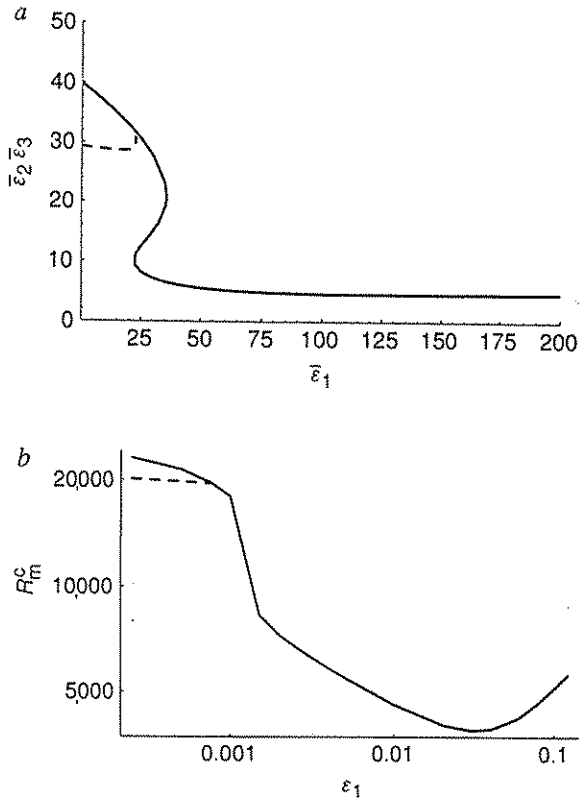

FIG. 1 Marginal stability curves as a function of meridian circulation. The lines give the critical dynamo parameters (see text for definitions of ε_1, $\bar{\varepsilon}_1$, $\bar{\varepsilon}_2$, $\bar{\varepsilon}_3$ and R_m^c) (solution neither grows nor decays): solid (dashed) lines denote steady (oscillatory) solutions. *a*, Braginsky limit $\alpha\omega$ system. *b*, 3D system, $\varepsilon_2 = \varepsilon_3 = 0.04$. When two solutions exist for one value of ε_1 ($\bar{\varepsilon}_1$), the one with smaller R_m^c ($\bar{\varepsilon}_2\,\bar{\varepsilon}_3$) is physically preferred.

The Braginsky asymptotic limit has, in this case, the complicated form: $\varepsilon_1 \to 0$, $R_m \to \infty$, $\bar{\varepsilon}_1 = \varepsilon_1 R_m = \text{constant}$, and $\varepsilon_2 \to 0$, $\varepsilon_3 \to 0$, $R_m \to \infty$, $\bar{\varepsilon}_2\bar{\varepsilon}_3 = \varepsilon_2\varepsilon_3 R_m = \text{constant}$. $R_m\alpha$ in equation (2) becomes replaced by $\bar{\varepsilon}_2\bar{\varepsilon}_3$. α And $\bar{\mathbf{v}}_{ep}$ may be calculated from the original flow as described by Braginsky[16] and are given for this case by Kumar and Roberts[23]; note that the effective meridian circulation means equation (2) contains a $\bar{\mathbf{v}}$ even in the Lilley case $\varepsilon_1 = 0$.

Figure 1*a* shows marginal stability curves for the Braginsky limit case; Fig 1*b* gives the corresponding 3D solutions. The oscillatory solution is preferred for $\varepsilon_1 \leqslant 0.0008$ ($\bar{\varepsilon}_1 \leqslant 22.5$). Roberts[17] conclusion for $\alpha\omega$ models, that meridian circulation promotes stationary solutions, is therefore confirmed in 3D, although we should strictly refer to 'effective meridian circulation' for the Braginsky limit results.

The radial component of the magnetic field at the core–mantle boundary for steady solutions exhibits flux concentrations (Fig. 2*a*, *b*) resembling those of the modern (1980) geomagnetic field

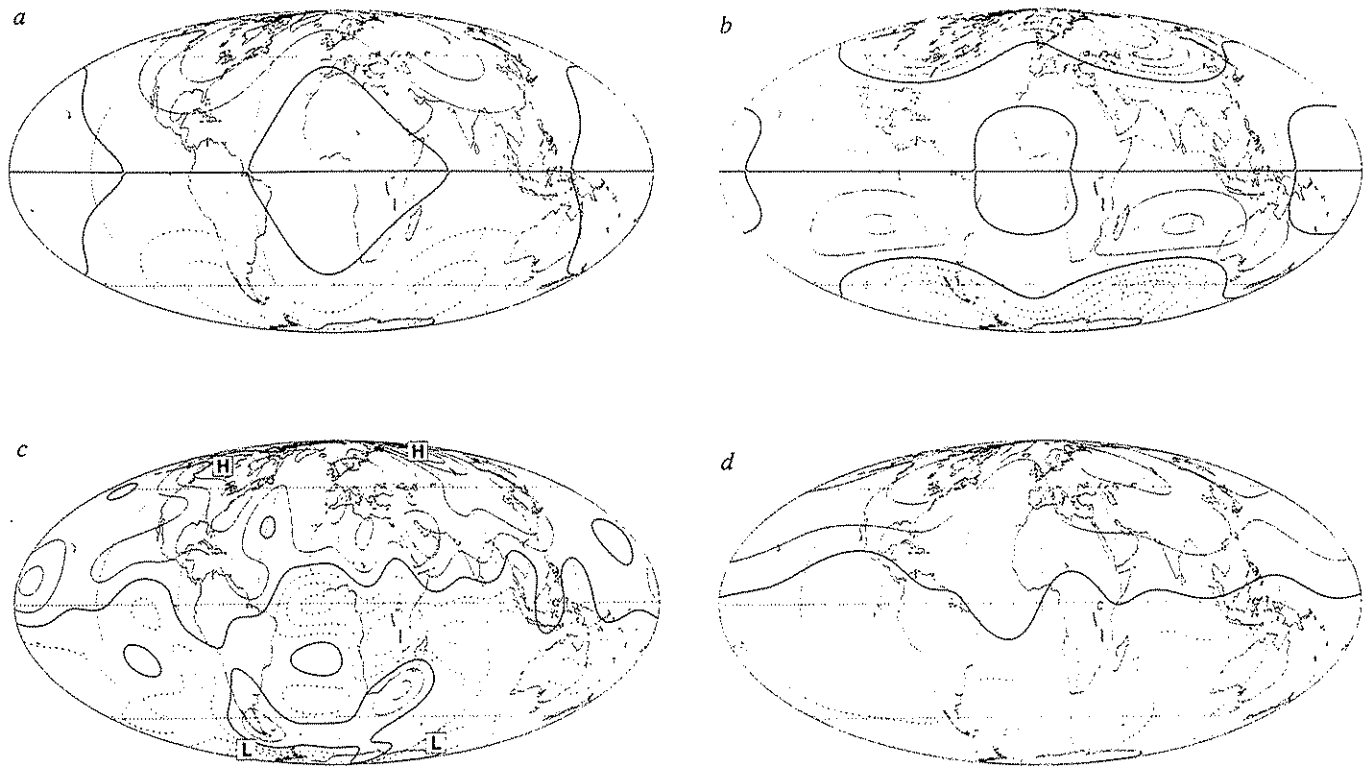

FIG. 2 Plots of the radial component of magnetic field (B_r) at the core–mantle boundary (CMB). *a*, For output of kinematic dynamo calculations for the Kumar and Roberts[23] velocity model, with $\varepsilon_1 = 0.03$, $\varepsilon_2 = \varepsilon_3 = 0.04$, a case previously studied by Kumar and Roberts. Magnetic flux is concentrated by fluid downwelling approximately along longitudes 90° W and 90° E and dispersed by upwelling along 0° and 180°, as discussed by Hutcheson and Gubbins[1]. *b*, For the same calculations, but using $\varepsilon_1 = 0.001$ *and* $\varepsilon_2 = \varepsilon_3 = 0.04$, a steady solution close to where the oscillatory solution takes over. The principal difference between this and a is the presence of reversed flux at low latitudes. *c*, For the modern (1980) geomagnetic field[28], for comparison with the kinematic output. Gubbins and Bloxham[28] pointed out that the four main geogmagnetic flux concentrations (marked H and L) are remarkably symmetric about the equator and positioned where convention rolls might intersect the core surface; our calculations confirm that convective downwelling could indeed produce such an effect. *d*, For the time-averaged palaeomagnetic field for the past 2.5 Myr (ref. 5), for comparision with flux concentrations of kinematic output. In *a–d*, solid (dashed) lines show concentrations of positive (negative) magnetic flux; bold lines show the zero contour. The axial dipole strengths are normalized to the present-day value of the geomagnetic dipole; contours are at 200-μT intervals. We include maps of the continents on our kinematic plots to facilitate comparison with the observed geomagnetic field; the positioning with respect to longitude is arbitrarily fixed by the definition of the velocity.

(Fig. 2*c*) and the time-averaged palaeomagnetic field for the past 2.5 Myr (ref. 5) (Fig. 2*d*). The positions of these flux patches can be related to the longitudes at which downwelling occurs in our velocity model[2], as might be anticipated from consideration of flux advection.

Figure 3 shows the surface field for the oscillatory solution in the Lilley case ($\varepsilon_1 = 0$). The morphology when the axial dipole component is strongest is very similar to that of the nearby steady solution. This solution has a period of approximately half the electromagnetic diffusion time—in geophysical terms a reversal time of ~5,000 years—and reverses by a dynamo wave mechanism[10].

We can compare the transition field morphology obtained from the dynamo model with that of the geomagnetic field. First note that a large region of reversed flux has grown in the past 100 years in the South Atlantic and Indian oceans[3] (Fig. 2*c*), suggestive of the reverse flux patches in the oscillatory solution (Fig. 3) and in nearby stationary solutions (Fig. 2*b*). Gubbins[3] has suggested that reversals may initiate in this way. Observed Virtual Geomagnetic Pole (VGP) transition paths seem to concentrate through the Americas, with a second preferred path through Asia[6,7,24,25]; this could be produced by migration of patches of reversed flux[26].

VGP transition paths are easy to calculate from the dynamo fields, and several are shown in Fig. 4; the paths tend to cluster along the two longitudes at which the main flux lobes of the field are concentrated, as might be intuitively expected, and as is observed for the Earth[25]. (This conclusion contrasts with that of Honkura *et al.*[27], who found no preferred longtitude bands for VGP paths calculated from a nonlinear dynamo model. We feel, however, that this model may have numerical convergence problems, and in any case the parameter values used are far from those expected in the Earth.)

With a transition field such as that in our model, two distinct paths arise not from different reversals but from different sites; the palaeomagnetist would see two bands, with any apparent preference caused by geographical bias of the sites. That such simple VGP paths can be so site-dependent should deter palaeomagnetists from drawing conclusions regarding the morphology of transition fields from analysis of VGP data alone; we emphasize the need for a good geographical spread in any database used to seek preferred paths. Clement[7], for example, has found two distinct paths from the same reversal recorded at different sites.

Geomagnetic reversals are not oscillations; they consist typically of one transition. Kinematic theory cannot simulate this behaviour—nonlinear calculations are required—but it might give a guide to possible nonlinear behaviour. If the dynamo were operating with a flow similar to those studied here, close to the steady–oscillatory boundary, its time variations

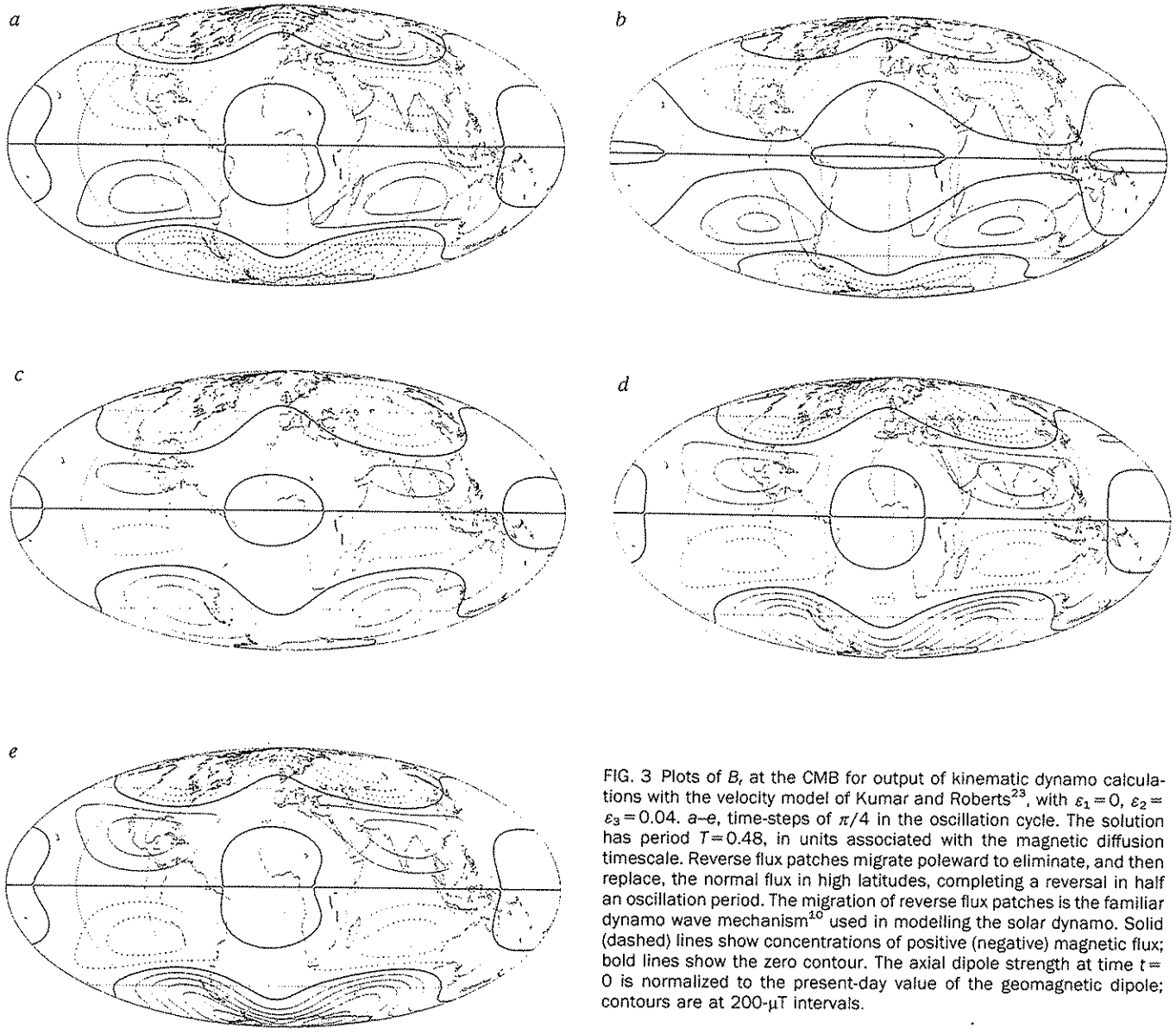

FIG. 3 Plots of B_r at the CMB for output of kinematic dynamo calculations with the velocity model of Kumar and Roberts[23], with $\varepsilon_1 = 0$, $\varepsilon_2 = \varepsilon_3 = 0.04$. *a*–*e*, time-steps of $\pi/4$ in the oscillation cycle. The solution has period $T = 0.48$, in units associated with the magnetic diffusion timescale. Reverse flux patches migrate poleward to eliminate, and then replace, the normal flux in high latitudes, completing a reversal in half an oscillation period. The migration of reverse flux patches is the familiar dynamo wave mechanism[10] used in modelling the solar dynamo. Solid (dashed) lines show concentrations of positive (negative) magnetic flux; bold lines show the zero contour. The axial dipole strength at time $t = 0$ is normalized to the present-day value of the geomagnetic dipole; contours are at 200-μT intervals.

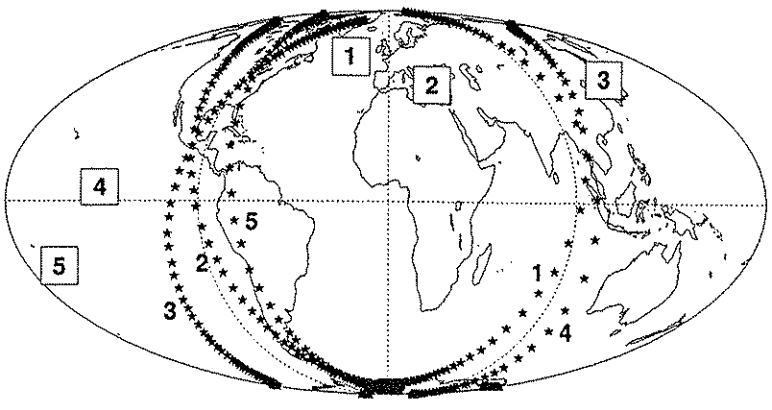

FIG. 4 Plot of synthetic Virtual Geomagnetic Pole (VGP) paths for the field models in Fig. 3 for five arbitrarily chosen sites. The figures in boxes mark and label the site locations; the smaller stars show the VGPs calculated for 301 equal time-steps in the course of one field reversal, with each path labelled by the appropriate site number. The paths are heavily site-dependent because the field does not reverse simply through an equatorial dipole: by the symmetry of the field, sites equatorially anti-symmetric or rotated 180° in longitude have antipodal paths: thus sites on the equator undergo an instantaneous reversal of the VGP. The approximate symmetry observed about the meridian plane $\phi = 0$ gives a similar effect: when the site is close to 0° or 180°, small changes in its longitude yield dramatic shifts of the transition path. Thus, an approximate quadrant-type behaviour is observed: sites approximately northeast or southwest of the point (0° N, 0° E) produce normal-to-reverse transition paths lying in one hemisphere, whereas sites in the remaining two quadrants produce an antipodal path.

might be expected to resemble a mix of the two field morphologies found here, and the reversal transition field would resemble the oscillatory solution.

Our mechanism differs from that of Parker and Levy[8-10], in which reversals are controlled by fluctuations in the latitude of the α effect rather than by strength of meridian circulation. So far no 3D solutions have been found for their case and no transition fields are available.

There are very few examples of geodynamo models that are sufficiently well developed to allow comparison with observation. We have found two simple physical effects that determine the field morphology and its time dependence: that downwelling causes concentration of flux and dynamo waves cause flux to migrate poleward. These effects are quite general and are expected to arise in a large range of dynamo models, both kinematic and dynamic. In combination they produce a striking effect: the VGP paths lie close to the longitudes of the flux concentrations of the neighbouring stationary fields. Some recent palaeomagnetic results[6,7] show this happening on the Earth, where the present-day flux concentrations reside near longitudes 90° W and 90° E, the same longitudes as outlined by many VGP reversal transition paths. □

Received 15 September 1993; accepted 17 January 1994.

1. Hutcheson, K. A. & Gubbins, D. *Geophys. J. Int.* **116,** 304–320 (1994).
2. Gubbins, D. in *Flow and Creep in the Solar System: Observations, Modelling and Theory* (eds Stone, D. B. & Runcorn, S. K.) 97–111 (Kluwer, Dordrecht, 1993).
3. Gubbins, D. *Nature* **326,** 167–169 (1987).
4. Merill, R. T. & McElhinny, M. W. in *The Earth's Magnetic Field: Its History, Origin and Planetary Perspective* Ch. 5 (Academic, San Diego, 1983).
5. Gubbins, D. & Kelly, P. *Nature* **365,** 829–832 (1993).
6. Tric, E. C. *et al. Phys. Earth planet. Inter.* **65,** 319–336 (1991).
7. Clement, B. M. *Earth planet. Sci. Lett.* **104,** 48–58 (1991).
8. Levy, E. H. *Astrophys. J.* **171,** 621–633 (1972).
9. Levy, E. H. *Astrophys. J.* **171,** 635–642 (1972).
10. Parker, E. N. in *Cosmical Magnetic Fields: Their Origin and Their Activity* Ch. 19 (Clarendon, Oxford, 1979).
11. Bullard, E. C. & Gellman, H. *Proc. R. Soc.* A**247,** 213–278 (1954).
12. Lilley, F. E. M. *Proc. R. Soc.* A**316,** 153–167 (1970).
13. Gibson, R. D. & Roberts, P. H. in *The Application of Modern Physics to the Earth and Planetary Interiors* (ed. Runcorn, S. K.) 577–602 (Wiley Interscience, New York, 1969).
14. Gubbins, D. *Phil. Trans. R. Soc.* A**274,** 493–521 (1973).
15. Dudley, M. L. & James, R. W. *Proc. R. Soc.* A**425,** 407–429 (1989).
16. Braginsky, S. I. *Soviet Phys. JET P* **20,** 726–735 (1965).
17. Roberts, P. H. *Phil. Trans. R. Soc.* A**271,** 663–697 (1972).
18. Moffatt, H. K. in *Magnetic Field Generation in Electrically Conducting Fluids* Ch. 9 (Cambridge Univ. Press, 1978).
19. Malkus, W. V. R. & Proctor, M. R. E. *J. Fluid Mech.* **67,** 417–443 (1975).
20. Jennings, R. L. & Weiss, N. O. *Mon. Not. R. astr. Soc.* **252,** 249–260 (1991).
21. Hagee, V. L. & Olson, P. *J. geophys. Res.* **96,** 11673–11687 (1991).
22. Hollerbach, R. & Jones, C. A. *Nature* **365,** 541–543 (1993).
23. Kumar, S. & Roberts, P. H. *Proc. R. Soc.* A**344,** 235–238 (1975).
24. Tric, E. C. *et al. J. geophys. Res.* **97,** 9337–9351 (1992).
25. Laj, C., Mazaud, A., Weeks, R., Fuller, M. & Herrero-Bervera, E. *Nature* **351,** 447 (1991).
26. Gubbins, D. & Coe, R. *Nature* **362,** 51–53 (1993).
27. Honkura, Y., Iijima, T. & Marsushima, M. *J. Geomag. Geoelectr.* **44,** 931–941 (1992).
28. Gubbins, D. & Bloxham, J. *Nature* **325,** 509–511 (1987).